Science of the Total Environment 621 (2018) 1023–1032

Contents lists available at ScienceDirect

Science of the Total Environment

journal homepage: www.elsevier.com/locate/scitotenv

Blowing dust and highway safety in the southwestern United States: Characteristics of dust emission "hotspots" and management implications

Junran Li [a,*], Tarek Kandakji [b], Jeffrey A. Lee [b], John Tatarko [c], John Blackwell III [a], Thomas E. Gill [d], Joe D. Collins [e]

[a] Department of Geosciences, The University of Tulsa, Tulsa, OK 74104, USA
[b] Department of Geosciences, Texas Tech University, Lubbock, TX 79409, USA
[c] Rangeland Resources and Systems Research Unit, USDA-ARS, Fort Collins, CO 80526, USA
[d] Department of Geological Sciences, University of Texas at El Paso, El Paso, TX 79968, USA
[e] Department of Science and Mathematics, Texas A & M University, San Antonio, TX 78224, USA

HIGHLIGHTS

- A total of 620 dust emission hotspots and their characteristics of land use were identified in the southwestern U.S.
- Location, timing, and magnitude of the dust production at the hotspots were identified.
- Fifty five hotspot sites are located within 1 km to adjacent highways.
- Thirteen hotspot sites could produce highly hazardous dust emissions to ground transportation with visibility <200 m.

GRAPHICAL ABSTRACT

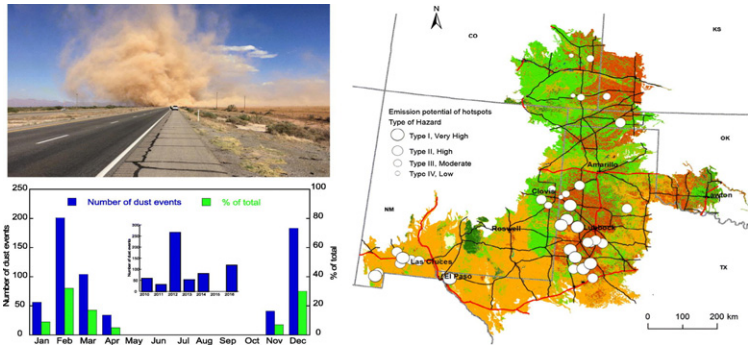

ARTICLE INFO

Article history:
Received 26 July 2017
Received in revised form 6 October 2017
Accepted 13 October 2017
Available online 6 November 2017

Editor: Simon Pollard

Keywords:
Land use
Highway management
Dust sources
Atmospheric dust
WEPS

ABSTRACT

Despite the widespread media attention of chain-reaction traffic incidents and property damage caused by wind-blown dust in the U.S. and elsewhere in the world, very few studies have provided in-depth analysis on this issue. Remote sensing and field observations reveal that wind erosion in the southwestern U.S. typically occurs in localized source areas, characterized as "hotspots", while most of the landscape is not eroding. In this study, we identified the spatial and temporal distribution patterns of hotspots that may contribute dust blowing onto highways in the southwestern U.S. We further classified the hotspots for the potential of blowing dust production based upon field observations and wind erosion modeling. Results of land use and land cover show that shrubland, grassland, and cropland accounted for 42%, 31%, and 21% of the overall study area, respectively. However, of the 620 total hotspots identified, 164 (26%), 141 (22%), and 234 (38%) are located on shrubland, grassland, and cropland, respectively. Barren land represented 0.9% of the land area but 8% of the dust hotspots. While a majority of these hotspots are located close to highways, we focused on 55 of them, which are located <1 km to adjacent highways and accessible via non-private roads. Field investigations and laboratory analysis showed that soils at these hotspot sites are dominated by sand and silt particles with threshold shear velocities ranging from 0.17–0.78 m s^{-1}, largely depending on the land use of the hotspot sites. Dust emission modeling showed that 13 hotspot sites could produce annual emissions >3.79 kg m^{-2}, yielding highly hazardous dust emissions to ground transportation with visibility <200 m. Results of location, timing, and magnitude of the dust production

* Corresponding author.
E-mail address: Junran@utulsa.edu (J. Li).

https://doi.org/10.1016/j.scitotenv.2017.10.124

at the hotspots are critical information for highway authorities to make informed and timely management decisions when wind events strike.

1. Introduction

The hazard of blowing dust to highway safety represents one of the significant impacts of aeolian processes on human welfare (Goudie, 2009; Baddock et al., 2013; Middleton, 2017).Goudie (2014) reported that dust-related fatal highway accidents happened in six states in the U.S. in 2012–2013. Earlier, Pauley et al. (1996) described a major incident in the San Joaquin Valley of California in 1991, where blowing dust led to 164 vehicles colliding and 168 dead or injured on U.S. Interstate Highway 5. Laity (2003) reported that dust mobilized from the Mojave River floodplain in California had caused fata highway accidents. In Arizona, Ladder et al. (2016) reported that dust storms are the third largest cause of weather fatalities and dust-related incidents have killed 157 and injured 1324 people over the last 50 years.Nationwide in the U.S., Ashley and Black (2008) found that dust events caused by non-convective wind storms alone contributed to 62 deaths between 1980 and 2005. Dust representing a highway hazard is not restricted to barren desert environments: wind erosion of agricultural lands also can cause deadly accidents. For example, Deetz et al. (2016) described an incident where windblown sediment from a nearby potato field caused a multi-fatality motor vehicle wreck on a German *autobahn*.

In addition, dust blowing across roads has a significant economic cost manifested in additional highway maintenance, shutdown of roads and detouring of traffic which impact logistics and timely delivery of goods and services as well as disrupting the conveyance of people (Goudie and Middleton, 1992; Baddock et al., 2013). The effect of dust on vehicle traffic thus represents one of the most significant "off-site" costs of wind erosion (Pimentel et al., 1995: Baddock et al., 2013). Despite the fact that blowing dust contributes to chain-reaction traffic incidents, delays in delivery, disrupts transportation schedules and causes and property damage every year in the U.S. and many other locations in the world, only a few studies have provided an in-depth analysis on the occurrence of such events, and little information is available to highway managers on the mitigation and management of this hazard.

From the "Dust Bowl" of the 1930s to the present, large areas of North America's Southern Great Plains, including northeastern New Mexico, western Oklahoma, western Texas, southeastern Colorado, and southwestern Kansas, have been noted for the occurrence of blowing dust (Lee and Tchakerian, 1995; Lee and Gill, 2015). The U.S. portion of the Chihuahuan Desert, extending from far eastern Arizona across southern New Mexico and far western Texas, is one of the most dust-prone regions in the Western Hemisphere (Prospero et al., 2002). Dust events in North American drylands may be driven by convective (mesoscale) or non-convective (synoptic-scale) windstorms (Novlan et al., 2007; Rivera Rivera et al., 2009). Remote sensing and field observations further revealed that dust in this region tends to emit from localized source areas associated with preferred land use, characterized as "hotspots", while most of the landscape does not erode (Gillette, 1999; Mahowald et al., 2005; Lee et al., 2009; Rivera Rivera et al., 2010; Lee et al., 2012) (Fig. 1). In western Texas and eastern New Mexico, Lee et al. (2009) found that most of the observable dust plumes originated on disturbed lands, such as cultivated cropland, and plumes of dust that emanate from individual point sources eventually merge into a shield-shaped region of dust.

It is widely recognized that blowing dust affects highway safety due to the reduction of visibility. Observations made by motorists also revealed that most of the dust events that were hazardous to highway safety were emitted from lands adjacent to the highway (Day, 1993). Blowing dust is primarily composed of particles with diameter less than 50 μm and is produced as a result of the saltation of sand-sized particles (50–500 μm in diameter) sandblasting the surface (Goudie and Middleton, 2006). In a typical dust-related traffic incident on the highway, suspension of dust-sized particles may cause the deterioration of visibility whereas the near-surface transport and deposition of saltation-sized particles may reduce the traction on the road surface.

The objectives of this study were two-fold: 1) to identify the spatial and temporal distribution patterns of hotspots that may contribute dust blowing to highways in the southwestern United States, and 2) to classify the hotspots for the potential of blowing dust production based upon field observations and wind erosion modeling. For this investigation, the study area was defined using United States Department of Agriculture Major Land Resource Areas (Austin, 1965) for the Southern High Plains and extending westward into known dust-producing regions in the Chihuahuan Desert of New Mexico, and northward into north Texas and the intersection areas of Texas, Oklahoma, Kansas, and Colorado (see Fig. 3).

2. Methods

2.1. Identification of dust emission hotspots

Lee et al. (2009, 2012) developed a methodology to identify dust sources and their associated geomorphic and land cover characteristics

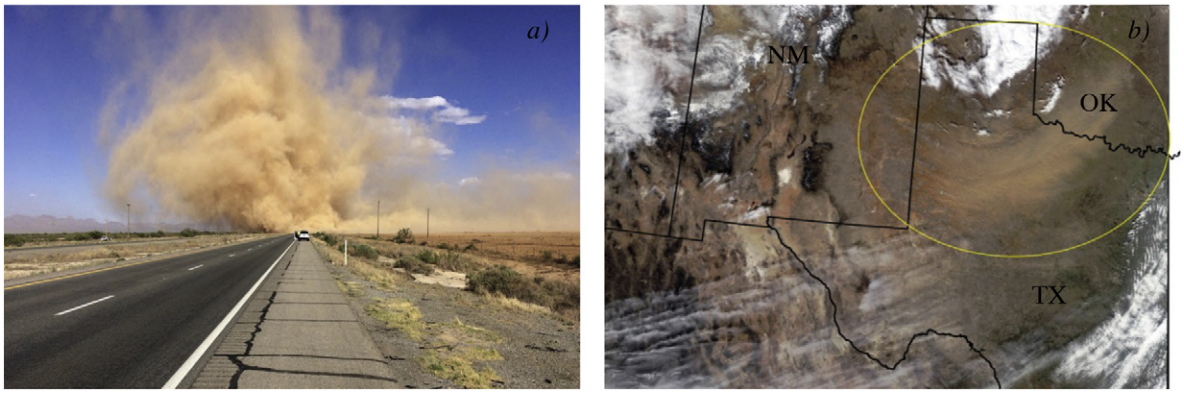

Fig. 1. Illustration of dust events in the southwestern U.S. *a*) example of blowing dust passing across a highway in San Simon, southeastern Arizona, May 16, 2016 (Source: CBS 5, Tucson, Arizona, 2016), and *b*) example of dust plumes shown on NASA's Aqua MODIS true color imagery in northern Texas, January 22, 2012.

in western Texas and New Mexico. In this method, meteorological records were used to determine the occurrence of airborne dust, and satellite images were used to identify dust sources. Days for image analysis were determined when the visibility dropped to 5 km or less for at least 1 h. The meteorological data were obtained from the U.S. National Weather Service at 15 representative cities within the study area. The dust sources were further identified using the true color MODIS (Moderate Resolution Imaging Spectroradiometer) imagery for the period of 2010 to 2016. The imagery has a pixel size of 250 m.

To further improve the dust source identification, a "split-window" technique was applied to enhance the dust in scenes, based upon the brightness temperature difference between the MODIS thermal channels of 31 and 32 (Baddock et al., 2009). The resulting image has dust plumes enhanced as black, while water, ice, clouds, and ground surface show up as white. It is noteworthy that dust events would not be apparent in the imagery if cloud cover obscured the ground or the timing of the satellite overpasses in relation to the dust occurrence. Additionally, convective dust events (initiated by downdrafts from thunderstorms) generally cannot be resolved in MODIS imagery. Dust plumes were identified in each image and the latitude and longitude of the upwind origin of each plume were identified using the procedure developed by Bullard et al. (2009) and Lee et al. (2009).

Land cover map was obtained from the National Land Cover Dataset produced by the Multi-Resolution Land Characteristics Consortium (MRLC) (www.mrlc.gov). The latest database of NLCD 2011 was used. These land cover data are available at 30 m resolution and were derived primarily from Landsat images. We generally followed Level II of the U.S. Geological Survey land use and land cover classification system. The land cover map was overlaid with both the observed point sources and the highway distribution map to allow the determination of number of dust sources from each land cover type and their relative locations to the adjacent highways. For the purpose of this study, we focused on the interstate highways, U.S. numbered highways, and the parts of the state highways with speed limit >80 km/h (equivalent to 50 mph in the U.S. highway system).

In addition, we conducted a proximity analysis in ArcGIS (ArcGIS 10.3, Esri, Redlands, CA) to determine the distance of hotspots to the neighboring highways. The hotspots located within 1 km to adjacent highways were subject to further analysis described in the following sections.

2.2. Field verification, measurements, and laboratory analysis

A field campaign was conducted in June 2016 with the purpose to verify dust source remote sensing analysis, and to measure threshold shear velocity (TSV) of wind erosion on dust emission hotspots. TSV depicts the erodibility of soil surface and it is a key parameter in wind erosion observation and quantification. TSVs were estimated using a method developed by Li et al. (2010). In this method, TSV was quantitatively related with the resistance of the soil surface to disturbances created by a penetrometer and projectile shot by an air gun at the soil.A total of 10–15 repeated air gun and penetrometer measurements were conducted along three 50-m transects oriented at 100°, 220°, and 340° from due north at each hotspot location. At the time of TSV measurement, the volumetric soil water content was also measured using hand-held time-domain reflectometry (TDR 100, Spectrum Technologies Inc., Aurora, IL) with 12 cm probe rods. Finally, for shrubland and grassland hotspot sites, height and width of plant canopies along the transects were also recorded.

In the verification exercise, a total of 55 hotspots, located within 1 km to adjacent highways, were located and assessed with regard to land use/land cover, crop grown, irrigation, and surface conditions (e.g., crust, crop stems etc.). These hotspot sites were accessible via non-private roads. In addition, for hotspots that are located close to each other but on the same land use (e.g., crop land), only one hotspot site was selected.

Finally, at each hotspot site, a composite soil sample was collected from the top 5-cm soil profile. Soil samples were processed and analyzed for texture and particle-size distribution using a laser diffraction Malvern Mastersizer 2000 particle-size analysis system (Malvern Instruments, Worcestershire, UK). For this analysis, we followed the protocols of Sperazza et al. (2004) and dispersed a subsample of approximately 0.9 g (obtained using a box splitter) in sodium hexametaphosphate solution and measured for grain size. Organic matter was not removed from the subsamples before the grain size analysis.

2.3. Simulation of dust emissions

Dust emissions from the hotspot sites were estimated using an up-to-date version of the Wind Erosion Prediction System (WEPS, v.1.5.52, released Nov 30, 2016). WEPS is a physical process-based daily time-step computer model that simulates weather, field surface conditions, and erosion (Wagner, 2013). WEPS was developed in the Great Plains environment of the U.S. and the model has been extensively validated in similar settings and elsewhere in the world (e.g. Hagen, 2004; Feng and Sharratt, 2007; Buschiazzo and Zobeck, 2008; Feng and Sharratt, 2009; Li et al., 2014).

The principal datasets that are required to run WEPS include soil properties, climate and wind, and crop management data. The physical dimensions (i.e., shape, area, length, and width) and the orientation of the hotspot sites were determined by using Google Earth™ images. No patterned barriers were observed at any of the hotspots. Climate and wind input files were generated within WEPS and reflect historical weather records. WEPS simulations were conducted using the cycle mode with a simulation cycle of 50 years for each year in the crop rotation (e.g., a two-year wheat-fallow rotation would have a simulation of 100 years). A minimum of 50 years per rotation year is needed to fully reflect historical weather distributions.

The distribution of crops and their rotations were determined using the USDA-NASS Cropland Data Layer (CDL). The CDL is a raster, georeferenced, land-cover dataset with a ground resolution of 30 m (NASS, 2015). The crop management files were obtained from the NRCS nationwide list of crop management zone files, which were developed by the NRCS based on typical crops and management practices employed on farms within each zone (Nelson et al., 2015).

Soil data was acquired from the USDA-NRCS Soil Survey Geographic (SSURGO) database and was downloaded via Simple Object Access Protocol (SOAP) from the NRCS Soil Data Mart website (NRCS, 2015).

WEPS simulations were conducted for all 55 field-verified hotspot sites located within 1 km to adjacent highways. Since suspension-size particles are the primary component of blowing dust, we reported flux of suspension particles and the time periods when the highest value of suspension was predicted by the WEPS model. WEPS considers particles <100 μm as suspension size.

It should be noted that WEPS was developed to simulate wind erosion on cropland, and appropriate adjustments must be made to the model's plant growth parameters and Management file in order to apply WEPS on non-cropland systems. For grasslands, we adjusted the generic "pasture" plant populations to represent those lands. For shrublands, we simulated a sparse perennial crop with parameters adjusted to grow similar plant geometry (i.e., canopy height, canopy width, fractional cover, leaf area index etc.) as found on shrublands in the study area, with the assumption that the shrubs are relatively uniformly distributed. For sites on both land uses, we also excluded tillage, harvest, irrigation etc., as they are not typically performed on grasslands and shrublands.

2.4. Classification of dust emission hotspots

For hotspots that are close to the highways, the amount of airborne dust, M, that is generated from an area of A during a wind event with

duration of T, may be estimated as:

$$M = F \times T \times A \quad (1)$$

where F isdust emission (also called vertical dust flux) that represents the rate of particles that leave the surface area. F has a unit of mass per unit area per time and was estimated using the WEPS model for individual hotspot sites.

For a short period of time after the dust entrainment, the concentration of dust in the air (C_d, g m^{-3}) may be calculated as:

$$C_d = \frac{M}{A' \times H} \quad (2)$$

where A' is the area of the dust plume when it travels to the highway, and H is the height of the dust plume. For dust plumes that are relatively close to the source areas, we assumed $A' = A$, and $H = 100$ m for a blowing dust event with strong wind.

Finally, visibility, V (m), is related to the concentration of dust in the air according to an equation developed by Patterson and Gillette (1977):

$$V^{\gamma} = \frac{C}{C_d} \quad (3)$$

where C and γ are empirical constants. For western Texas, Patterson and Gillette (1977) reported that the best values were $C = 2.0 \times 10^{-2}$ g m^{-3} km and $\gamma = 1.07$, when visibility measurements were made close to the dust source (e.g., <10 km).Using this method in combination with other field observations (e.g., Hagen and Skidmore, 1977; Baddock et al., 2014), we developed a visibility classification system related to concentrations of dust in the air (Perry and Symons, 2002) (Table 1). The visibility and associated dust in the air were used to classify the hotspots based upon their hazardous dust production potential simulated by the WEPS.

3. Results

3.1. Distribution of the hotspots

For the period of 2010–2016, a total of 620 dust emission hotspots were identified and located. Dust events associated with these hotspots are highly seasonal (Fig. 2). More than 50% of the dust events occurred from February to March and nearly 40% occurred from November to December. No dust events were identified from May to October during our study period. Annually, the year of 2012 had notably higher number of dust events than the rest of the years. Data for 2015 was not available as we were not able to obtain cloud-free MODIS images for the study area at the times of dust events.

In the study area, the primary land use classes include shrubland (42%), grassland (31%), and cultivated crop (21%, hereafter called cropland) (Table 2). The spatial distribution of the hotspots and their associated types of land use in the study area were shown in Fig. 3 and Appendix 1. Of the 620 total hotspots, 164 (26%), 141 (22%), and 234 (38%) are located on shrubland, grassland, and cropland, respectively (Table 2). Also note that barren land represents 0.9% of the study area, but 8% of the dust hotspots. These hotspots are generally centralized

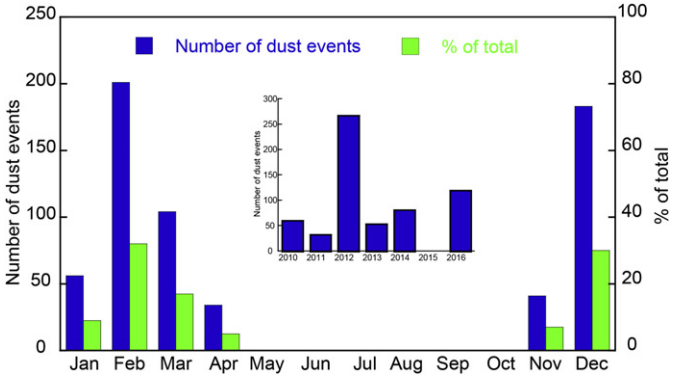

Fig. 2. The temporal distribution of the dust events that were associated with dust emission hotspots identified during the period of 2010–2016 in the study area. Note the 2015 data was missing because no cloud-free MODIS images were obtained.

in three primary regions: north region (north of Interstate Highway I-40), south-central region (centralized in the Lubbock, Texas and Clovis, New Mexico area, including part of the Interstate Highways I-40 and I-27), and the Chihuahuan Desert region (centralized in the El Paso-Las Cruces-Deming area with the primary Interstate Highways I-10 and I-25). In the north region, most of the dust sources occurred on grassland and cropland, whereas in south-central region, a majority of the dust sources were located on the cropland. Finally in the Chihuahuan Desert region, nearly all dust sources were found on shrubland.

The buffering analysis showed that of the 620 total dust emission hotspots, 75 (or 12%) are located less than 1 km to adjacent highways (Fig. 4), and these hotspots are located primarily in the south-central region (Fig. 5). Among these hotspots, 8 are located close to interstate highways (e.g., I-10), and 67 are located close to local highways. Fig. 4 also shows that more than 70% of the hotspots are located within 10 km of a nearby highway in our study area.

3.2. Dust emission potentials from the hotspots

Soils at the hotspot sites that are located within 1 km to adjacent highways are dominated by sand and silt particles, despite the fact that they are located on different types of land use (Fig. 6, Appendix 1). Except for the hotspot sites that are located on barren sandy land, soils at the hotspots generally have abundant supply of fine particles, e.g., particles with diameter of 50–100 μm, giving them a greater potential of generating dust plumes from wind erosion.

Threshold shear velocities (TSVs) for the surface soil at individual hotspot sites and different types of land use in the study area are show in Fig. 7 and Appendix 1. These results show that TSVs on the different types of land use are not significantly different, except for the barren land, which has significantly lower TSVs than those of the other types of land use. Fig. 7b also shows that disturbed soils could have much higher potential to produce blowing dust than that of the undisturbed soils (e.g., surface protected by physical or biological soil crust), illustrated by significantly higher TSVs. For example, average TSVs for undisturbed and disturbed playa sites are 1.15 m s^{-1} and 0.35 m s^{-1}, respectively. At the time of TSV measurement, soil water content at the hotspot sites was moderate and varied from 5% to 20% (data not shown).

Table 1
A visibility classification system that was used to classify dust emission hotspots to highway traffic.

Visibility	Concentration of dust in the air (mg m^{-3})	Levels of hazard to highway traffic	Comparable to foggy conditions[a]
<200 m	>110	I, Very high	Dense-thick fog
200 m–1 km	20–110	II, High	Fog-thick fog
1 km–2 km	5–20	III, Moderate	Mist, haze
2 km −5 km	1–5	IV, Low	Poor visibility
>5 km	<1	V, Not affected	Good visibility

[a] According to Perry and Symons (2002).

Table 2
Land cover category in the study area and the associated distribution of dust emission hotspots.

Land use class	Area (km^2)	Area (%)	Dust source points (n)	Dust source point (%)
Scrub/shrubland	164,386.4	41.6	161	25.9
Grassland	123,582.7	31.2	133	21.5
Cultivated crop/cropland	81,577.8	20.6	238	38.4
Urban/built environment	11,666.4	2.9	28	4.5
Forest	8862.8	2.2	5	0.8
Barren land	3498.9	0.9	48	7.7
Wetlands	1215.8	0.3	3	0.5
Open water	829.7	0.2	4	0.7

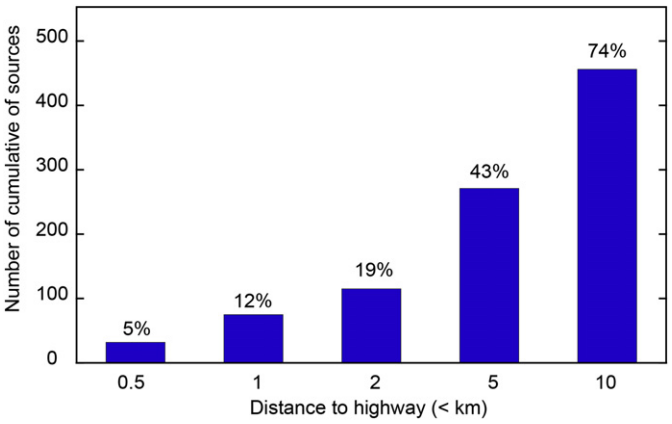

Fig. 4. Distribution of the dust emission hotspots relative to adjacent highways. Numbers on top of each bar indicate the cumulative percent of hotspots as the distance increases.

WEPS simulations show that among the 55 hotspot sites that are located within 1 km to adjacent highways, 13 have the potential to produce annual dust emissions >3.79 kg m^{-2}. These hotspots fall in the Type I (Very High) hazard to highway traffic in the study area (Fig. 8, Appendix 1). Among these hotspots, 8 are located in the south-central region with associated land use of cropland and 2 are found in the Chihuahuan Desert region on shrubland. The simulation results further revealed that the highest likelihood that these hotspots will produce hazardous blowing dust is in February and March (Appendix 1).

Up to 21 hotspots were classified to Type II (High) hazard to highway traffic, with estimated annual dust emission of 4.81–0.76 kg m^{-2}. Among these hotspots, 14 are located in the south-central region, 6 are located in the Chihuahuan Desert region, and 1 is located in the northern region (Fig. 8, Appendix 1). The reminder of the 55 hotspots that are close to the highways were classified to have Type III (Moderate) to Type V (Not Affected) hazard to highway traffic, including a few hotspots that occurred on grassland and cropland in the north region of the study area.

4. Discussion

Despite the widespread media attention of chain-reaction traffic incidents and property damage caused by windblown dust in the U.S. and elsewhere in the world, very few studies have investigated the relation of accident rates to windblown dust.

4.1. Distribution of the dust emission hotspots

Results show that dust events and associated dust emission hotspots in our study area had strong temporal and spatial patterns (Figs. 2, 3).

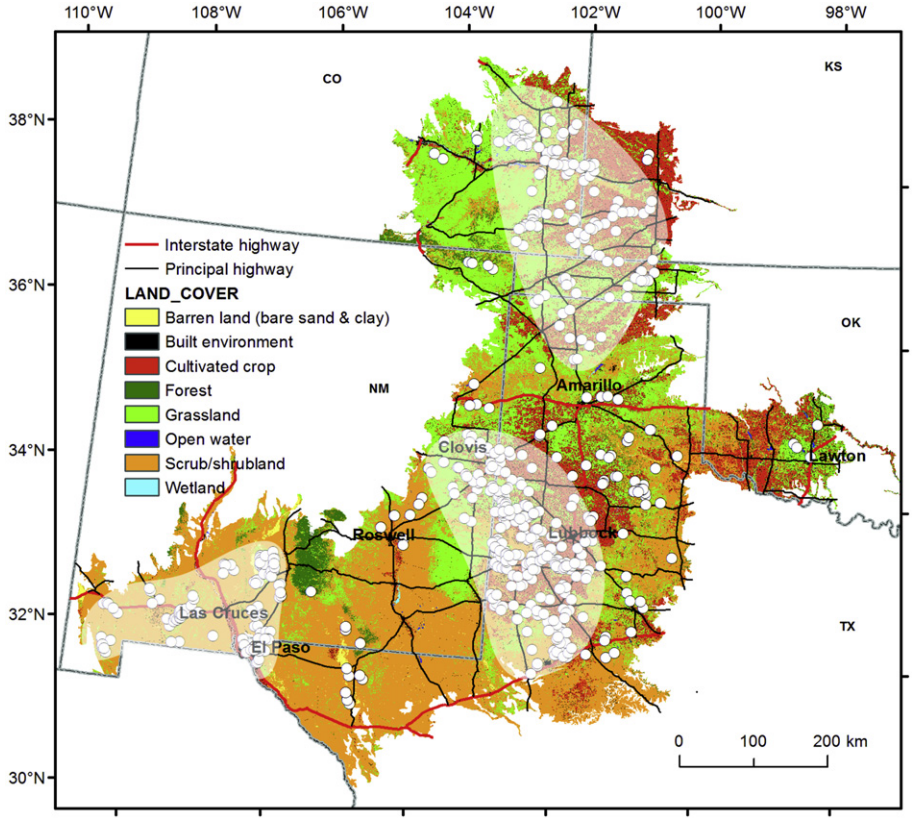

Fig. 3. The spatial distribution of the 620 dust emission hotspots (white circles), the associated land use on the surface, and their relative locations to the highways in the study area. The shaded areas are the approximate distribution of the three primary dust emission hotspot regions.

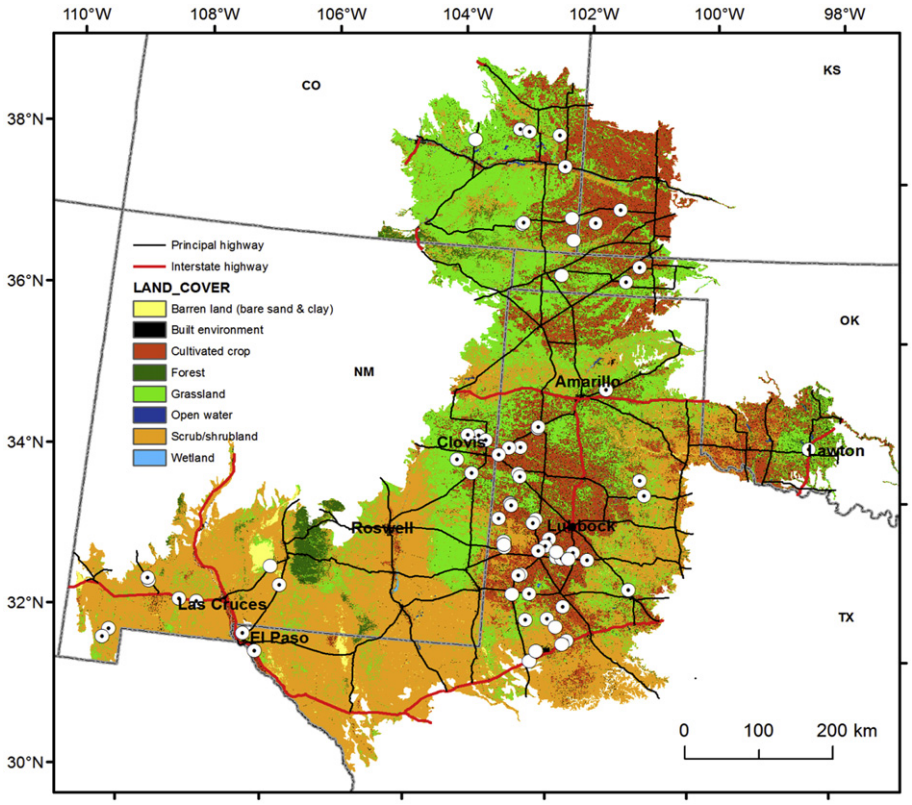

Fig. 5. The spatial distribution of dust emission hotspots that are located within 1 km to the adjacent highways. White dotted circles denote the 55 hotspot sites where field verification and investigation were conducted. These are also the sites where the blowing dust emission potential was evaluated by WEPS modeling.

Nearly 90% of the dust events occurred in spring (Feb–Mar) and winter (Nov–Dec), and substantially more dust events were identified in 2012, a year when extensive drought occurred in the southwestern U.S. (Hoerling et al., 2014). The temporal pattern of dust emission hotspots identified by this study is well in line with long-term field observations for two primary cities in the study area, i.e., Lubbock, Texas (Lee et al., 1994), and El Paso, Texas (Novlan et al., 2007).Similar to the temporal patterns, about 88% of the dust sources are located on the three primary types of land use, cropland, shrubland, and grassland. However, the fact that cropland, which occupies 21% of the land use in the study area but produced 38% of the total hotspots suggests that cropland produces proportionately more dust than both grassland and shrubland. Barren land is an even more disproportionate dust producer, as it occupies less than 1% of the study area but produced almost 8% of the total hotspots. This is consistent with the findings of a previous study using a different set of remote sensing data (Rivera Rivera et al., 2010) that the barren land class is a disproportionate source of hazardous dust events impacting major cities in the region.

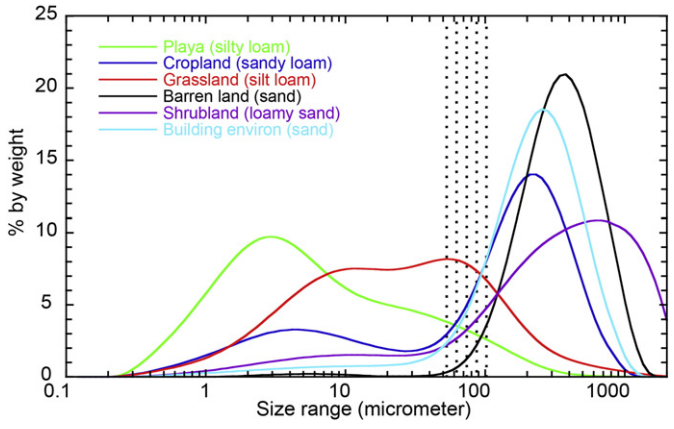

Fig. 6. Particle-size distribution of soils from representative dust emission hotspots located at different land uses identified in this study. Dotted area indicates range of soil particle size which is generally found to have lower threshold shear velocity and therefore is more susceptible to dust emission (Marticorena and Bergametti, 1995).

4.2. Potential limitations of the dust source identification method

Identification and cataloging of dust emission hotspots in a region allows for improved numerical modeling of the evolution of individual dust plumes and better forecasting of the onset and end of dust storm conditions, therefore representing a first step to manage and mitigate hazardous blowing dust for highway safety. Various approaches, including frequency statistics, model simulation, and remote sensing, have been developed to identify dust emission sources (e.g., Ginoux et al., 2001; Prospero et al., 2002; Rivera Rivera et al., 2010; Park et al., 2010; Parajuli et al., 2014). These approaches, each with its own advantages and weaknesses, are largely constrained by the availability of the data (e.g., model input data, remote sensing imagery etc.) and the geographic scale of the research area.

In this study, we focused on the dust emissions from individual locations, i.e., hotspots, and their potential hazard to ground transport. We visually identified sources of dust emission on satellite images, aided by meteorological records and proved quality improvement techniques. This method, however, has some known limitations (Lee et al., 2009, Rivera Rivera et al., 2010; Lee et al., 2012). Most notably, because dust obscures the ground, dust sources beneath the dust cloud (i.e., downwind of the source) may not be detected, whereas upwind sources may be preferentially identified by this approach. In the case of this study, most dust events were associated with westerly or southwesterly wind (the prevailing wind direction in the study area: Lee et al., 1994; Novlan et al., 2007), so western, upwind sources were

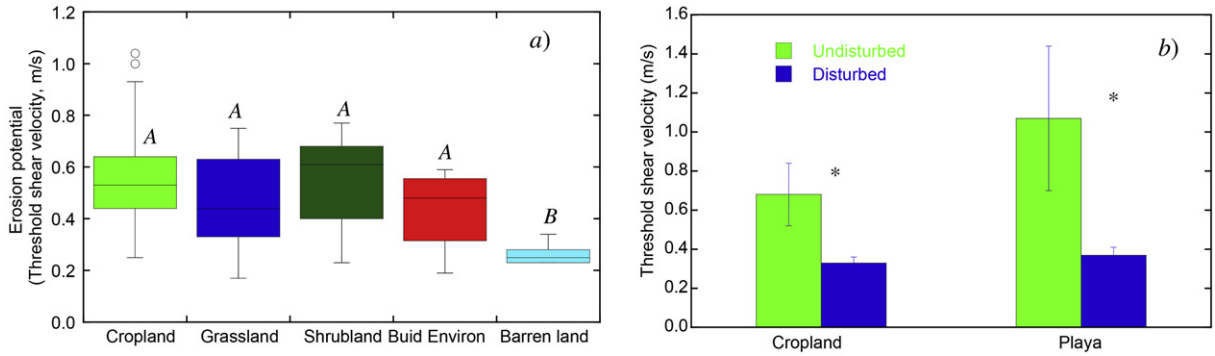

Fig. 7. Characteristics of threshold shear velocity (TSV) of surface soil measured from primary land use in the study area. *a*) Box plot of TSV, *b*) TSV for disturbed and undisturbed surfaces. Different letters and * indicate significant difference ($p < 0.05$) between different land uses by ANOVA for *a*) and *t*-test for *b*), respectively.

more likely to be identified. Additionally, precise location of source points is somewhat subjective because dust in 'true color' scenes is similar to the underlying ground surface. Lee et al. (2009) also pointed out that because erosion may occur before there is sufficient downwind plume development to make the plume observable in the image, the exact source points of some plumes may have been located a small distance upwind of where the 250 m MODIS pixel first indicated the presence of dust. Finally, some dust activity is likely missed due to the relative timing of overpass and dust emissions as the satellites with MODIS aboard only pass twice per day. Despite the fact that the overall method for identifying the point sources for the event is less than perfect, it is arguably the best method available for the purpose of our study (Baddock et al., 2009).

4.3. Dust emission potential at the hotspots

Although more than 600 dust emission hotspot sites were identified, their potential to produce hazardous blowing dust to affect highway traffic is not equal. Numerous studies have shown that the dust events that deteriorate visibility and therefore jeopardize motorists are associated with preferred land use types that are close to the highway (e.g., Day, 1993; Pauley et al., 1996, Lee et al., 2009). Accordingly, we prioritized the large number of dust emission hotspots to 55 based on their distance to the adjacent highway (i.e., <1 km) and accessibility. Although TSVs and particle-size distribution for soils located at many of these hotspot sites are largely similar, WEPS modeling showed that their potential of blowing dust emission is notably different. Very

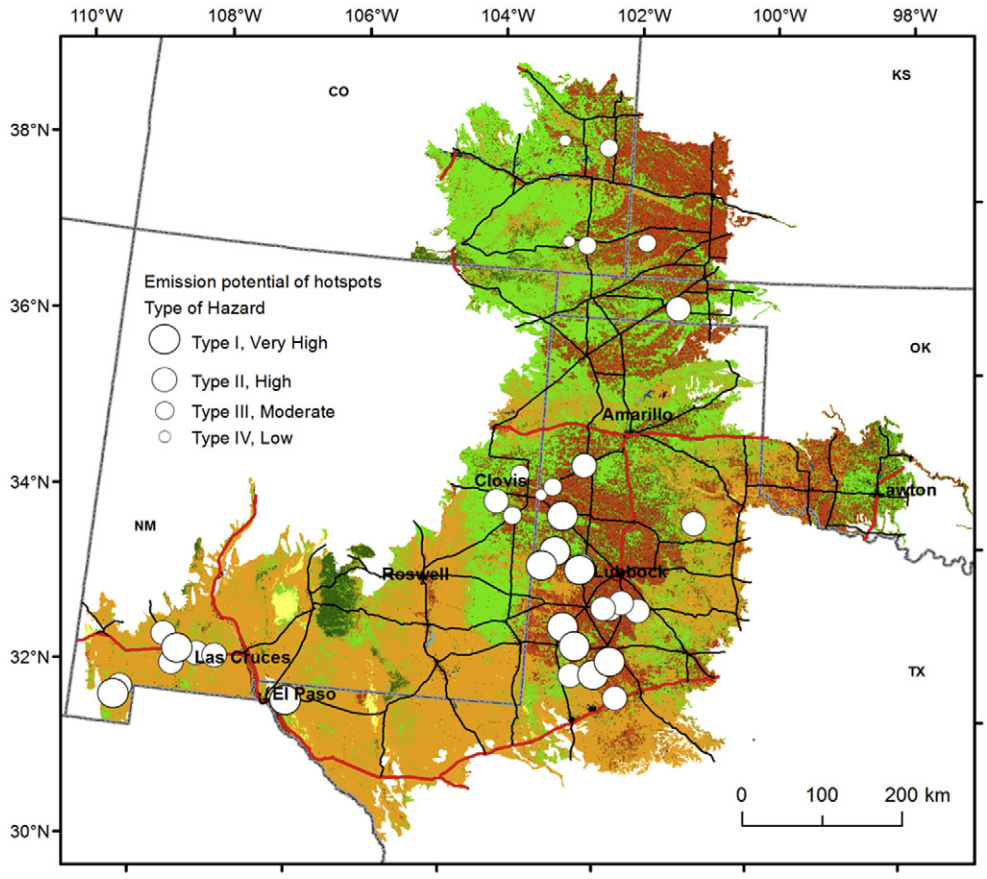

Fig. 8. Distribution of dust emission hotspots with different potential to produce hazardous blowing dust on the highway. Types of hazardous blowing dust are defined in Table 1 and the magnitudes of WEPS simulated suspension at the hotspot sites are listed in Appendix 1. Note the Type V (Not Affected) hotspots were not shown on the map.

importantly, in combination with an empirical equation of visibility and particle concentration, we further identified a number of hotspot sites with which close attention must be paid on blowing dust production. Among these hotspots, 13 of them have the highest potential to produce hazardous blowing dust, with the magnitude that could reduce the visibility to <200 m in certain periods of February and March. The localities of these hotspots illustrated the significance of cropland(in the central, Great Plains region) and shrubland (in the southwestern, Chihuahuan Desert region) on dust production. In the northern and central study areas, most cropland use is devoted to cotton farming and the local farming techniques leave the soil bare from November to May (Lee et al., 1994; Nordstrom and Hotta, 2004). Lee et al. (1994) also showed that in this period of time strong winds are common and are generally from west and southwest. The location, timing, and magnitude of the dust production at the hotspots are critical information for highway authorities to make informed and timely management decisions when wind events strike.

Dust emission hotspots that are located >1 km away from neighboring highways, although are not specifically investigated in this study, may also contribute hazardous dust to highway traffic. In the southwestern U.S. and many other arid environments in the world, dust plumes that emanate from individual point sources may merge into a large-scale, shield-shaped region of dust (i.e., Darmenova et al., 2005; Miller et al., 2006; Lee et al. 2009).This large aerosol shield, once passing across a highway, may pose a serious threat to transportation safety.

4.4. Management implications

The rank of the dust emission hotspots to highway safety, however, is not static. Our TSV measurements suggest that dust emission may increase substantially if the soil surface is disturbed or the vegetation cover is lost. This is a particular concern for playas or sites where the physical soil crust may be disturbed by recreational vehicles, cattle grazing and trampling, land use change etc. While TSVs of the hotspot sites were only measured once in our study, they are well-known to vary over time due to changes of soil moisture (Li et al., 2015). Nevertheless, the combination of strong winds and unvegetated, loose sediments in spring and early summer makes these areas highly active hotspots for dust production (Gillette, 1999; Lee et al., 2009; Rivera Rivera et al., 2010). A case in point is the Lordsburg Playa, crossed by Interstate Highway I-10, located near the border of New Mexico and Arizona. Blowing dust has been frequently observed crossing the highway from the surface of the Playa (Fig. 9) where the soil and vegetation has been disturbed by human activities (Department of the Interior, 1998) and natural flooding events (Scuderi et al., 2010). This blowing dust has caused numerous fatal multi-vehicle traffic accidents on I-10 in recent years, including 10 persons killed in dust-related crashes in 2017 alone (Associated Press, 2017).

Also in southwestern New Mexico, blowing dust has caused road closures and accidents on a mile-long stretch of U.S. 180, about 24 km northwest of Deming. The Department of Transportation of New Mexico has planned to use netting and reseeding to promote vegetation growth on this denuded pasture to reduce hazardous driving conditions created by blowing dust (Associated Press, 2016). Our study identified multiple dust emission hotspots along this highway, and furthermore, the WEPS simulations revealed that this area may be subject to Type I to II scale of dust events during the time of February and March (Fig. 8).

Climate projections suggest that mid-latitude continental interiors of the U.S., including a large portion of the southwestern U.S., will experience warmer and drier conditions (Seager et al., 2007; Diffenbaugh et al., 2008). As a result, soil moisture in summer is projected to be 15–20% lower, and more frequent and persistent droughts are expected (Easterling et al., 1997; Cook et al., 2015). In fact, many of the Great Plains states have experienced multi-year droughts recently (Hoerling et al., 2014) and the impact of the drought on wind erosion has been manifested by the escalated number of dust events observed in 2012 in our study area (Fig. 2). Long-term data show that the frequency of dust storms is already increasing (Tong et al., 2017) and the length of the dust storm season is already expanding (Hand et al., 2016) in Southwest North America. A most recent study suggested that projected climate change, along with enhanced land surface bareness, will likely bring more frequent and extreme dust activity to the southern Great Plains in the U.S. (Pu and Ginoux, 2017), and therefore activate some of the low-rank hotspots identified in this study.

5. Conclusions

A total of 620 dust emission hotspots were identified in the Southern Great Plains and part of the Chihuahuan Desert of the southwestern U.S. from 2010 to 2016, and these sources primarily occurred on cropland and shrubland.Overlaying the distribution of the hotspots and the highway systems, we found that many of these dust sources are located close to highways, and therefore could contribute harmful blowing dust to the ground transportation. Although TSVs and particle-size distribution for soils located at many of these hotspot sites are largely similar, WEPS modeling showed that the potential of blowing dust emission is notably different, primarily due to land use type. Accordingly, we prioritized the large number of dust emission hotspots to 55 based on their distance to the adjacent highway (i.e., <1 km) and accessibility for field study. Although the WEPS model cannot pinpoint the intensity of individual dust events and the exact timing of their occurrence, results of this study still have important implications for highway authorities to make informed management decisions. Knowing the locations of dust emission hotspots and their potential to produce hazardous blowing dust will also provide a baseline for land managers, as these are the

Fig. 9. A scene of dust plumes intersecting Interstate 10 highway near Lordsburg Playa, New Mexico. Looking east across the Playa, March 22, 2016 (Source: T. Gill).This stretch of road has been the site of dozens of traffic fatalities in dusty conditions.

locations where human interventions need to be exercised with the greatest care. These locations may also be especially susceptible to future climate and land use change. Findings of our study represent a first step to ultimately develop an integrated modeling and monitoring system to mitigate the hazardous impacts of dust on highway safety in the U.S. and elsewhere in the world.

Supplementary data to this article can be found online at https://doi.org/10.1016/j.scitotenv.2017.10.124.

Acknowledgements

This research was supported by the U.S. Department of Transportation Southern Plains Transportation Center Grant SPTC14.1-39. We thank Kagan Richard for additional field and laboratory assistance. Both the data from the experiments, input files necessary to reproduce the graphs and photographs from the field site are included as a supplement to the manuscript and are also available from the authors upon request (junran@utulsa.edu).

References

Ashley, W.S., Black, A.W., 2008. Fatalities associated with nonconvective high-wind events in the United States. J. Appl. Meteorol. Climatol. 47, 717–725.
Associated Press, 2016. State plans steps to reduce blowing dust on US 180. http://www.lcsun-news.com/story/news/2016/11/29/state-plans-steps-reduce-blowing-dust-us-180/94625100/ (accessed 17.06.08).
Associated Press, 2017. 2 killed in freeway crash in NM dust storm. http://www.lcsun-news.com/story/news/local/2017/02/24/2-killed-freeway-crash-nm-dust-storm/98369206/ (accessed 17.05.10).
Austin, M.E., 1965. Land resource regions and major land resource areas of the United States (exclusive of Alaska and Hawaii). USDA Agricultural Handbook. 296.
Baddock, M.C., Bullard, J.E., Bryant, R.G., 2009. Dust source identification using MODIS: a comparison of techniques applied to the Lake Eyre Basin, Australia. Remote Sens. Environ. 113, 1511–1528.
Baddock, M.C., Strong, C.L., Murray, P.S., McTainsh, G.H., 2013. Aeolian dust as a transport hazard. Atmos. Environ. 71, 7–14.
Baddock, M.C., Strong, C.L., Leys, J.F., Heidenreich, S.K., Tews, E.K., McTainsh, G.H., 2014. A visibility and total suspended dust relationship. Atmos. Environ. 89, 329–336.
Bullard, J.E., Harrison, S.P., Drake, N., Gill, T.E., 2009. Preferential dust sources in global aerosol models: a new classification based on geomorphology. Eos. Trans. AGU 90 (52 Suppl) (EP23D-01).
Buschiazzo, D.E., Zobeck, T.M., 2008. Validation of WEQ, RWEQ and WEPS wind erosion for different arable land management systems in the Argentinean pampas. Earth Surf. Process. Landf. 33:1839–1850. https://doi.org/10.1002/esp.1738.
CBS 5, Tucson, Arizona, 2016. I-10 reopens after being closed again for blowing dust. http://www.walb.com/story/31986701/i-10-reopens-after-being-closed-again-for-blowing-dust (accessed 17.05.10).
Cook, B.I., Ault, T.R., Smerdon, J.E., 2015. Unprecedented 21st century drought risk in the American Southwest and Central Plains. Sci. Adv. 1 (1), e1400082.
Darmenova, K., Sokolik, I.N., Darmenov, A., 2005. Characterization of east Asian dust outbreaks in the spring of 2001 using ground-based and satellite data. J. Geophys. Res. 110:D02204. https://doi.org/10.1029/2004JD004842.
Day, R.W., 1993. Incidents on interstate highways caused by blowing dust. J. Perform. Constr. Facil. 7 (2), 128–132.
Deetz, K., Klose, M., Kirchnerand, I., Cubasch, U., 2016. Numerical simulation of a dust event in northeastern Germany with a new dust emission scheme in COSMO-ART. Atmos. Environ. 126, 87–97.
Department of Interior, Bureau of Land Management, NM-030-1220-00, 1998. Emergency Closure of the Lordsburg Playa to Off-Highway Vehicles (OHV), Hidalgo County, NM. Federal Register (USA). 63 p. 34661 (122).
Diffenbaugh, N.S., Giorgi, F., Pal, J.S., 2008. Climate change hotspots in the United States. Geophys. Res. Lett. 35, L16709.
Easterling, W.E., Hays, C.J., Easterling, M.M., Brandle, J.R., 1997. Modeling the effect of shelterbelts on maize productivity under climate change: an application of the EPIC model. Agric. Ecosyst. Environ. 61, 163–176.
Feng, G., Sharratt, B., 2007. Validation of WEPS for soil and PM10 loss from agricultural fields within the Columbia Plateau of the United States. Earth Surf. Process. Landf. 32:743–753. https://doi.org/10.1002/esp.i434.
Feng, G., Sharratt, B., 2009. Evaluation of the SWEEP model during high wind on the Columbia plateau. Earth Surf. Proc. Land. 34:1461–1468. https://doi.org/10.1002/esp.1818.
Gillette, D.A., 1999. A qualitative geophysical explanation for "hotspot" dust emitting source regions. Contrib. Atmos. Phys. (Beiträge zur Physik der Atmosphäre) 72 (1), 67–77.
Ginoux, P., Chin, M., Tegen, I., Prospero, J., Holben, B., Dubovik, O., Lin, S., 2001. Sources and distributions of dust aerosols simulated with the GOCART model. J. Geophys. Res.-Atmos. 106 (D17):20255–20273. https://doi.org/10.1029/2000JD000053.
Goudie, A.S., 2009. Dust storms: recent development. J. Environ. Manag. 90:89–94. https://doi.org/10.1016/j.jenvman.2008.07.007.
Goudie, A.S., 2014. Desert dust and human health disorders. Environ. Int. 63, 101–113.
Goudie, A.S., Middleton, N.J., 1992. The changing frequency of dust storms through time. Clim. Chang. 20, 197–225.
Goudie, A.S., Middleton, N.J., 2006. Desert Dust in the Global System. Springer-Verlag, Heidelberg, Germany.
Hagen, L.J., 2004. Evaluation of the wind erosion prediction systems (WEPS) erosion submodel on cropland fields. Environ. Model. Softw. 19, 171–176.
Hagen, L.J., Skidmore, E.L., 1977. Wind erosion and visibility problem. Trans. ASAE 20 (5), 898–903.
Hand, J.L., White, W.H., Gebhart, K.A., Hyslop, N.P., Gill, T.E., Schichtel, B.A., 2016. Earlier onset of the spring fine dust season in the southwestern United States. Geophys. Res. Lett. 43 (8), 4001–4009.
Hoerling, M., Eischeid, J., Kumar, A., Leung, R., Mariotti, A., Mo, K., Schubert, S., Seager, R., 2014. Causes and predictability of the 2012 Great Plains drought. Bull. Am. Meteorol. Soc. 95 (2), 269–282.
Lader, G., Raman, A., Davis, J.T., Waters, K., 2016. Blowing dust and dust storms: one of Arizona's most underrated weather hazards. NOAA Technical Memorandum NWS-WR. 290.
Laity, J., 2003. Aeolian destabilization along the Mojave River, Mojave Desert, California: linkages among fluvial, groundwater and aeolian systems. Phys. Geogr. 24, 196–221.
Lee, J.A., Gill, T.E., 2015. Multiple causes of wind erosion in the dust bowl. Aeolian Res. 19: 15–36. https://doi.org/10.1016/j.aeolia.2015.09.002.
Lee, J.A., Tchakerian, V.P., 1995. Magnitude and frequency of blowing dust on the southern High Plains of the United States, 1947–1989. Ann. Assoc. Am. Geogr. 85, 684–693.
Lee, J.A., Allen, B.L., Peterson, R.E., Gregory, J.M., Moffett, K.E., 1994. Environmental controls on blowing dust direction at Lubbock, Texas, USA. Earth Surf. Process. Landf. 19, 437–449.
Lee, J.A., Gill, T.E., Mulligan, K.R., Dominguez, M.A., Perez, A.E., 2009. Land use/land cover and point sources of the 15 December 2003 dust storm in southwestern North America. Geomorphology 105, 18–27.
Lee, J.A., Baddock, M.C., Mbuh, M.J., Gill, T.E., 2012. Geomorphic and land cover characteristics of aeolian dust sources in west Texas and eastern New Mexico, USA. Aeolian Res. 3 (4):459–466. https://doi.org/10.1016/j.aeolia.2011.08.001.
Li, J., Okin, G.S., Herrick, J.E., Belnap, J., Munson, S.M., Miller, M.E., 2010. A simple method to estimate threshold friction velocity of wind erosion in the field. Geophys. Res. Lett. 37, L10402. https://doi.org/10.1029/2010GL043245.
Li, J., Okin, G.S., Tatarko, J., Webb, N.P., Herrick, J.E., 2014. Consistency of wind erosion assessments across land use and land cover types: a critical analysis. Aeolian Res. 15: 253–260. https://doi.org/10.1016/j.aeolia.2014.04.007.
Li, J., Flagg, C., Okin, G.S., Painter, T.H., Dintwe, K., Belnap, J., 2015. On the prediction of threshold friction velocity of wind erosion using soil reflectance spectroscopy. Aeolian Res. 19, 129–136.
Mahowald, N.M., Baker, A.R., Bergametti, G., Brooks, N., Duce, R.A., Jickells, T.D., Kubilay, N., Prospero, J.M., Tegen, I., 2005. Atmospheric global dust cycle and iron inputs to the ocean. Glob. Biogeochem. Cycles 19:GB4025. https://doi.org/10.1029/2004GB002402.
Marticorena, B., Bergametti, G., 1995. Modeling the atmospheric dust cycle: 1. Design of a soil-derived dust emission scheme. J. Geophys. Res. 100 (16), 415–16,430.
Middleton, N.J., 2017. Desert dust hazards: a global review. Aeolian Res. 24:53–63. https://doi.org/10.1016/j.aeolia.2016.12.001.
Miller, S.D., Hawkins, J.D., Lee, T.F., Turk, F.J., Richardson, K., Kuciauskas, A.P., Kent, J., Wade, R., Skupniewicz, C.E., Cornelius, J., O 'Neal, J., Haggerty, P., Sprietzer, K., Legg, G., Henegar, J., Seaton, B., 2006. MODIS provides a satellite focus on Operation Iraqi Freedom. Int. J. Remote Sens. 27, 1285–1296.
NASS-National Agricultural Statistics Service, U.S. Department of Agriculture, 2015. CropScape Geospatial Portal. Available at:. http://nassgeodata.gmu.edu/CropScape/, Accessed date: 15 June 2017.
Nelson, R., Tatarko, J., Ascough II, J.C., 2015. Soil erosion and organic matter variations for central Great Plains cropping systems under residue removal. Trans. ASABE 58 (2), 415–427.
Nordstrom, K.F., Hotta, S., 2004. Wind erosion from cropland in the USA: a review of problems solutions and prospects. Geoderma 121 157–157.
Novlan, D.J., Hardiman, M., Gill, T.E., 2007. A synoptic climatology of blowing dust events in El Paso, Texas from 1932–2005. Preprints, 16th Conference on Applied Climatology. American Meteorological Society, p. 12 J3.
NRCS, Soil data mart, USDA Natural Resources Conservation Service, 2015. Web Soil Survey. Available at. http://websoilsurvey.nrcs.usda.gov, Accessed date: 20 June 2017.
Parajuli, S.P., Yang, Z.L., Kocurek, G., 2014. Mapping erodibility in dust source regions based on geomorphology, meteorology, and remote sensing. J. Geophys. Res. 119: 1977–1994. https://doi.org/10.1002/2014JF003095.
Park, S.U., Choe, A., Lee, E.H., Park, M.S., Song, X., 2010. The Asian dust aerosol model 2 (ADAM2) with the use of normalized difference vegetation index (NDVI) obtained from the Spot4/vegetation data. Theor. Appl. Climatol. 101, 191–208.
Patterson, E.M., Gillette, D.A., 1977. Measurements of visibility vs mass-concentration for airborne soil particles. Atmos. Environ. 11, 193–196.
Pauley, P.M., Baker, N.L., Barker, E.H., 1996. An observational study of the "Interstate 5" dust storm case. Bull. Am. Meteorol. Soc. 77, 693–720.
Perry, A.H., Symons, L.J., 2002. Highway meteorology. E & FN SPON, p. 208.
Pimental, D., Harvey, C., Resosudarmo, P., Sinclair, K., Kurz, D., McNair, M., Crist, S., Shpritz, L., Fitton, L., Saffouri, R., Blair, R., 1995. Environmental and economic costs of soil erosion and conservation benefits. Science 267, 1117–1123.
Prospero, J.M., Ginoux, P., Torres, O., Nicholson, S.E., Gill, T.E., 2002. Environmental characterization of global sources of atmospheric soil dust identified with the Nimbus 7 Total Ozone Mapping Spectrometer (TOMS) absorbing aerosol product. Rev. Geophys. 40, 1002:2002. https://doi.org/10.1029/2000RG000095.
Pu, B., Ginoux, P., 2017. Projection of American dustiness in the late 21st century due to climate change. Sci Rep 7:5553. https://doi.org/10.1038/s41598-017-05431-9.

Rivera Rivera, N.I., Gill, T.E., Gebhart, K.A., Hand, J.L., Bleiweiss, M.P., Fitzgerald, R.M., 2009. Wind modeling of Chihuahuan Desert dust outbreaks. Atmos. Environ. 43, 347–354.
Rivera Rivera, N.R., Gill, T.E., Bleiweiss, M.P., Hand, J.L., 2010. Source characteristics of hazardous Chihuahuan Desert dust outbreaks. Atmos. Environ. 44, 2457–2468.
Scuderi, L.A., Laudadio, C.K., Fawcett, P.J., 2010. Monitoring playa lake inundation in the western United States: modern analogues to late-Holocene lake level change. Quat. Res. 73, 48–58.
Seager, R., et al., 2007. Model projections of an imminent transition to a more arid climate in southwestern North America. Science 316, 1181–1184.
Sperazza, M., Moore, J.N., Hendrix, M.S., 2004. High-resolution particle size analysis of naturally occurring very fine-grained sediment through laser diffractometry. J. Sediment. Res. 74:736–743. https://doi.org/10.1306/031104740736.
Tong, D.Q., Wang, J.X., Gill, T.E., Lei, H., Wang, B., 2017. Intensified dust storm activity and valley fever infection in the southwestern United States. Geophys. Res. Lett. 44 (9), 4304–4312.
Wagner, L.E., 2013. A history of wind erosion prediction models in the United States Department of Agriculture: the wind erosion prediction system (WEPS). Aeolian Res. 10, 9–24.